

Shaping up BPS States with Matrix Model Saddle Points

Diego H. Correa and Martin Wolf* †

*Department of Applied Mathematics and Theoretical Physics
University of Cambridge
Wilberforce Road, Cambridge CB3 0WA, United Kingdom*

Abstract

We provide analytical results for the probability distribution of a family of wavefunctions of a quantum mechanics model of commuting matrices in the large- N limit. These wavefunctions describe the strong coupling limit of $1/8$ BPS states of $\mathcal{N} = 4$ supersymmetric Yang–Mills theory. In the large- N limit, they should be dual to classical solutions of type IIB supergravity that asymptotically approach $\text{AdS}_5 \times S^5$. Each probability distribution can be described as the partition function of a matrix model (different wavefunctions correspond to different matrix model potentials) which we study by means of a saddle point approximation. These saddle point solutions are given in terms of (five-dimensional) hypersurfaces supporting density distributions of eigenvalues.

29th July 2010

*Also at the Wolfson College, Barton Road, Cambridge CB3 9BB, United Kingdom.

†*E-mail addresses:* d.correa@damtp.cam.ac.uk, m.wolf@damtp.cam.ac.uk

Contents

1. Introduction	1
2. Quantum mechanics of commuting matrices	3
2.1. Wavefunctions	3
2.2. Large- N limit	4
3. Analytical solutions	7
3.1. Perturbative expansions	7
3.2. Example A: Monomial deformations	9
3.3. Example B: Logarithmic deformations	13
4. Conclusions and outlook	17
Appendices	
A Eigenvalues and eigenfunctions	18
B Jacobi polynomials	21

1. Introduction

Since the discovery of the anti-de Sitter space/conformal field theory (AdS/CFT) correspondence [1], significant progress has been made in our understanding of strongly coupled gauge theory phenomena. So far, the example that has been studied most extensively is the correspondence between $SU(N)$ maximal $\mathcal{N} = 4$ supersymmetric Yang–Mills (SYM) theory in four dimensions and type IIB superstring theory on the ten-dimensional $AdS_5 \times S^5$ background. The correspondence in its strongest form claims full dynamical agreement between both theories at the quantum level. This is certainly hard to verify and one therefore seeks limits in which it is possible to perform tests explicitly. One very interesting limit is the planar or large- N limit of the gauge theory. In this limit, $\mathcal{N} = 4$ SYM theory is believed to be equivalent to free (i.e. genus-zero) string theory on $AdS_5 \times S^5$. If one in addition assumes strong 't Hooft coupling (or equivalently, large curvature radius of AdS), then the gauge theory is believed to be described by classical supergravity.

One may adopt the point of view of taking the AdS/CFT correspondence as an approach towards defining a theory of quantum gravity. This then naturally leads to the question of how geometrical information emerges in the strong coupling limit of the gauge theory. Notice that gravity is not apparent in the Lagrangian description of quantum field theory and in this sense it can be thought of as ‘emergent’. Moreover, the gravity side of the correspondence is higher dimensional, therefore one should also be able to understand how excitations are localised in the dual extra dimensions by field theoretical means.

To shed light on the problem of emergent geometry, one needs to study strongly coupled gauge theory, which on general grounds, is extremely hard. To tackle this problem, Berenstein [2] proposed a truncation of $\mathcal{N} = 4$ SYM to a quantum mechanical problem of commuting matrices by compactifying the theory on a three-sphere (i.e. he considered $\mathcal{N} = 4$ SYM theory on $\mathbb{R} \times S^3$). This compactification provides a natural infra-red regulator. Moreover, upon expanding all the fields of $\mathcal{N} = 4$ SYM theory in spherical harmonics on the three-sphere, the action is truncated to obtain a quantum mechanics Hamiltonian of six Hermitian matrices. This truncation of the degrees of freedom to commuting matrices is a good approximation in the strong coupling limit.¹

¹The notion of emergent geometry in the strong coupling limit of more general matrix models was studied in [3].

The eigenstates of the model with six commuting matrices are conjectured to describe 1/8 BPS states of $\mathcal{N} = 4$ SYM theory at strong coupling. In the large- N limit, these are dual to classical solutions of type IIB supergravity that asymptotically approach $\text{AdS}_5 \times S^5$. Similar models have been proposed to describe BPS states in orbifolds of $\mathcal{N} = 4$ SYM theory [4] and certain $\mathcal{N} = 1$ superconformal field theories [5].

A Gaussian wavefunction of the eigenvalues of the commuting matrices was shown to be the exact ground state of the quantum mechanical Hamiltonian [2]. The product of this ground state by a holomorphic function of the matrices' eigenvalues is an eigenfunction of the Hamiltonian, as well, at least to a good approximation in the large- N limit [5, 6]. Now, having this family of quantum mechanical eigenstates, it would be desirable to characterise their typical or most likely distribution of eigenvalues. The probability distribution of each of the wavefunctions can be seen as the partition function of a given matrix model. For the ground state, the resulting partition function would be that of a model with a quadratic potential and a generalised Vandermonde repulsion. For the 'excited' wavefunctions, other terms are added to the potential of the model. In the large- N limit, all these partition functions will be dominated by their saddle points. Although only for the ground state the saddle point equations have been solved exactly so far [2, 7], the result is very compelling: The saddle point configuration is a uniform distribution of eigenvalues supported on a five-sphere embedded into \mathbb{R}^6 . Just to remind the reader, the ground state wavefunction must be identified with the dual of the $\text{AdS}_5 \times S^5$ background. Subsequent studies revealed that it is possible to confer an explicit geometrical interpretation to the five-sphere of eigenvalues [7]. In order to see if one can push this identification further, it would be necessary to compute the partition functions associated with other eigenstates of the quantum mechanical Hamiltonian. The simplest cases one could start from to look at are 1/2 BPS eigenstates. For these states the AdS/CFT dictionary has been studied thoroughly (see e.g. [8]) and it is known how to relate them to a family of 1/2 BPS supergravity solutions that asymptotically approach $\text{AdS}_5 \times S^5$, found by Lin, Lunin & Maldacena (LLM) [9]². Unfortunately, solving the corresponding partition functions in the quantum mechanics model with six commuting matrices is a very difficult problem, even in the saddle point approximation. The only reported results in this direction are in a series of articles that study some of these wavefunctions numerically for finite N [6, 12, 13].

In this paper, we will extend the analytical result that is known for the ground state wavefunction to excited wavefunctions. Specifically, we will develop a perturbative method that allows for an analytical treatment of the saddle point equations of a family of wavefunctions. We will present analytical results for monomial and logarithmic potentials in the corresponding matrix model Hamiltonian. Wavefunctions for degree $p \in \mathbb{N}$ monomial potentials are expected to be in correspondence with LLM geometries obtained from a simply connected droplet possessing a non-vanishing p^{th} harmonic moment [10]. Wavefunctions for logarithmic potentials should correspond to annular LLM geometries where the inner radius is determined by the strength of the logarithmic potential [2]. Our results should form a starting point for extracting geometric information directly from the gauge theory. We will comment on this issue in the conclusions.

This paper is organised as follows. We will first give a brief review of the background material. In Section 3., we then provide our perturbative approach and present analytical solutions for monomial and logarithmic potentials. We shall also compare our results against the numerics. In Section 4., we will conclude and give an outlook of open problems. Finally, several appendices collect useful definitions and details of our derivations.

²An alternative approach to recast geometrical information of LLM solutions was used in [10, 11].

2. Quantum mechanics of commuting matrices

The system we are going to be dealing with is a particular matrix quantum mechanics model of six commuting Hermitian matrices. Let $\vec{X} = (X^1, \dots, X^6)$ be the six Hermitian matrices, they are therefore subject to the constraint

$$\vec{X} \wedge \vec{X} = 0. \quad (2.1)$$

The Hamiltonian we are interested in is

$$H^{\text{cl}} = \frac{1}{2} \text{tr}(\vec{\Pi} \cdot \vec{\Pi} + \vec{X} \cdot \vec{X}), \quad (2.2)$$

where $\vec{\Pi}$ is conjugate to \vec{X} and ‘cl’ refers to classical. The system has a gauge invariance, where one acts by conjugation: $\vec{X} \mapsto g^{-1} \vec{X} g$ for $g \in \text{SU}(N)$. Because of the constraint (2.1), one can use this $\text{SU}(N)$ action to diagonalise all six matrices \vec{X} simultaneously. Let us denote the eigenvalues of \vec{X} by $\vec{x}_i = (x_i^1, \dots, x_i^6) \in \mathbb{R}^6$ for $i, j, \dots = 1, \dots, N$. Having diagonalised all the matrices, we have fixed a gauge. However, there are still residual gauge transformations which permute the eigenvalues \vec{x}_i . Therefore, the corresponding wavefunctions will eventually be symmetric under the exchange $\vec{x}_i \leftrightarrow \vec{x}_j$ for all i and j .

As shown by Berenstein [2], this system can be obtained as a truncation of $\mathcal{N} = 4$ SYM theory on $\mathbb{R} \times S^3$, to the s -wave modes of its six scalar fields, to describe gauge invariant $1/8$ BPS states in the strong coupling limit.

Having reduced the dynamics of these six $N \times N$ matrices to the dynamics of their eigenvalues, the system can thus be interpreted as set of N bosons on a space with six dimensions. If we treat the system classically, we can use a diagonal ansatz to find solutions of the dynamical system. Under these assumptions, we find N free harmonic oscillators in six dimensions, which should be treated as N identical particles (bosons) on a six-dimensional harmonic oscillator.

Quantum mechanically, we cannot do that immediately. This is due to a certain measure factor that arises from the volume of the gauge orbit, and which affects the dynamics of the system. This measure factor was computed in [2] and it is given by

$$\mu^2 := \prod_{1 \leq i < j \leq N} |\vec{x}_i - \vec{x}_j|^2. \quad (2.3)$$

The resulting quantum Hamiltonian is therefore

$$H = \sum_{i=1}^N \left(-\frac{1}{2\mu^2} \vec{\nabla}_i \cdot \mu^2 \vec{\nabla}_i + \frac{1}{2} |\vec{x}_i|^2 \right). \quad (2.4)$$

2.1. Wavefunctions

The main object of study in this paper will be some wavefunctions of the Hamiltonian (2.4). The presence of the Vandermonde measure factor makes the corresponding Schrödinger problem very difficult. Notice nonetheless that the rather simple wavefunction

$$\psi_0(\vec{x}_1, \dots, \vec{x}_N) = \exp\left(-\frac{1}{2} \sum_{i=1}^N |\vec{x}_i|^2\right) \quad (2.5)$$

is an exact wavefunction of H . In fact, it is the ground state wavefunction,

$$H\psi_0 = E_0\psi_0, \quad \text{with} \quad E_0 = \frac{N}{2}(N-1) + 3N. \quad (2.6)$$

The measure factor μ , which will appear in the probability density distribution, can be absorbed into the wavefunction ψ by a similarity transformation

$$\psi \mapsto \hat{\psi} := \mu\psi . \quad (2.7)$$

In the following, we shall concern ourselves with the re-scaled wavefunctions $\hat{\psi}$ only.

If we square $\hat{\psi}$, we get a probability density distribution on the phase space of the N particles. For the ground state $\hat{\psi}_0$, this is given by

$$|\hat{\psi}_0|^2 = \mu^2 \exp\left(-\sum_{i=1}^N |\vec{x}_i|^2\right) = \exp\left(-\sum_{i=1}^N |\vec{x}_i|^2 + \sum_{1 \leq i < j \leq N} \log |\vec{x}_i - \vec{x}_j|^2\right) . \quad (2.8)$$

If we set $\mathcal{H}_0 := -\log |\hat{\psi}_0|^2$, then

$$\mathcal{Z}_0 = \int \left(\prod_{i=1}^N d^6 x_i\right) \exp(-\beta \mathcal{H}_0) , \quad \text{with } \beta \equiv 1 \quad (2.9)$$

can be interpreted as the partition function of a gas of particles in a confining external quadratic potential, $\sum_i |\vec{x}_i|^2$, together with a logarithmic repulsion term, $-\sum_{i < j} \log |\vec{x}_i - \vec{x}_j|^2$, between the particles in six dimensions.³

Less is known about the exact excited wavefunctions for the Hamiltonian H . However, in [2,6] it was shown that for 1/2 BPS states, the wavefunction

$$\hat{\psi}_f(\vec{x}_1, \dots, \vec{x}_N) := \exp\left(\sum_{i=1}^N f(z_i)\right) \hat{\psi}_0(\vec{x}_1, \dots, \vec{x}_N) \quad (2.10)$$

is an approximate eigenfunction of H in the thermodynamic limit $N \rightarrow \infty$, provided $f = f(z_i)$ is a holomorphic function of $z_i := x_i^5 + ix_i^6$. The partition function in this case is then given by

$$\mathcal{Z}_f = \int \left(\prod_{i=1}^N d^6 x_i\right) \exp(-\beta \mathcal{H}_f) , \quad \text{with } \beta \equiv 1 , \quad (2.11a)$$

where

$$\mathcal{H}_f := -\log |\hat{\psi}_f|^2 = \sum_{i=1}^N |\vec{x}_i|^2 - 2 \sum_{i=1}^N \Re f(z_i) - \sum_{1 \leq i < j \leq N} \log |\vec{x}_i - \vec{x}_j|^2 . \quad (2.11b)$$

Here, ‘ \Re ’ denotes the real part.

In this work, we shall be interested in the large- N limit of the ‘matrix model’ partition function (2.11a). In this limit, the bosons will form some type of distribution density ρ on the phase space of a single particle (density of eigenvalues). The goal for us is then to determine the shape of the density ρ using a saddle point approximation.

2.2. Large- N limit

Next we wish to perform the thermodynamic limit of the Hamiltonian (2.11b). When taking the limit $N \rightarrow \infty$, we may trade the sums in \mathcal{H}_f for integrals at the expense of introducing a density $\rho = \rho(\vec{x})$ (which is constrained to be non-negative),

$$\sum_{i=1}^N \rightarrow \int d^6 x \rho(\vec{x}) \quad \text{and} \quad \sum_{1 \leq i < j \leq N} \rightarrow \frac{1}{2} \int d^6 x d^6 x' \rho(\vec{x}) \rho(\vec{x}') , \quad (2.12a)$$

³This logarithmic repulsion generalises the Vandermonde repulsion of eigenvalues in matrix models of [14].

and which is subject to the normalisation

$$\int d^6x \rho(\vec{x}) = N . \quad (2.12b)$$

Therefore, (2.11b) becomes

$$\mathcal{H}_f = \int d^6x \rho(\vec{x}) |\vec{x}|^2 - 2 \int d^6x \rho(\vec{x}) \Re f(z) - \frac{1}{2} \iint d^6x d^6x' \rho(\vec{x}) \rho(\vec{x}') \log |\vec{x} - \vec{x}'|^2 . \quad (2.13)$$

Notice that the constraint (2.12b) might be added to (2.13) by using a Lagrange multiplier Λ .

In the large- N limit, the partition function (2.11a) will be dominated by its saddle point. Then, the most likely density ρ can then be obtained by extremising the Hamiltonian \mathcal{H}_f . Specifically, the variation of \mathcal{H}_f with respect to ρ yields

$$\Lambda + |\vec{x}|^2 - 2 \Re f(z) - \int d^6x' \rho(\vec{x}') \log |\vec{x} - \vec{x}'|^2 = 0 , \quad (2.14)$$

where the constraint (2.12b) is enforced by Λ . This is the integral equation that determines the density ρ . Upon acting with Δ^3 on this equation, where Δ is the Laplacian on \mathbb{R}^6 , one quickly realises that ρ cannot be an ordinary function but must be of distributional support [2].⁴ Thus, the integral equation (2.14) can only hold in a suitable region of \mathbb{R}^6 . In particular, for the ground state where $f = 0$, the density ρ is uniformly supported on a five-sphere $S^5 \subset \mathbb{R}^6$ [2, 7].

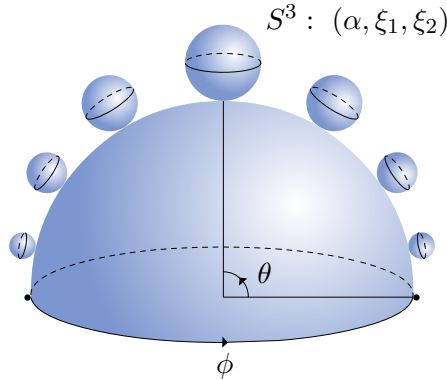


Figure 1: Five-sphere described by the spherical coordinates (2.15) (for fixed r): The hemisphere is parametrised by $\omega = (\theta, \phi)$ while the three-spheres are parametrised by (α, ξ_1, ξ_2) . Notice that the radii of the three-spheres shrink to zero as θ approaches zero.

Instead of Cartesian coordinates (x^1, \dots, x^6) , we will find it fruitful to make use of the following spherical parametrisation of $\mathbb{R}^6 \setminus \{0\}$:

$$\begin{aligned} x^1 &= r \sin \theta \sin \alpha \sin \xi_1 , & x^2 &= r \sin \theta \sin \alpha \cos \xi_1 , & x^3 &= r \sin \theta \cos \alpha \sin \xi_2 , \\ x^4 &= r \sin \theta \cos \alpha \cos \xi_2 , & x^5 &= r \cos \theta \cos \phi , & x^6 &= r \cos \theta \sin \phi , \end{aligned} \quad (2.15)$$

with $\theta, \alpha \in [0, \pi/2]$ and $\phi, \xi_{1,2} \in [0, 2\pi)$. Notice that with this choice of coordinates, we have

$$z = x^5 + ix^6 = r \cos \theta e^{i\phi} . \quad (2.16)$$

To proceed we should make an ansatz for the density ρ . We will take it to be supported on a hypersurface in \mathbb{R}^6 . Then, since in all the cases we consider the potential deformation $f = f(z)$

⁴In this argument, one uses the fact that $\Delta_x^3 \log |\vec{x} - \vec{x}'| \sim \delta^{(6)}(\vec{x} - \vec{x}')$.

depends only on the holomorphic coordinates z , we propose the following ansatz for the density ρ :

$$\rho(\vec{x}) = \frac{N}{2\pi^2 \hat{r}(\theta, \phi)^5} \delta(r - \hat{r}(\theta, \phi)) \hat{\rho}(\theta, \phi) . \quad (2.17)$$

Here, $\hat{\rho} = \hat{\rho}(\theta, \phi)$ and $\hat{r} = \hat{r}(\theta, \phi)$ are non-negative functions which depend only on θ and ϕ and δ indicates Dirac's delta function. The problem of finding the density ρ has thus been translated into finding the functions $\hat{\rho}$ and \hat{r} . Notice that the constraint (2.12b) then becomes

$$\int_0^{\pi/2} d\theta \int_0^{2\pi} d\phi \cos \theta \sin^3 \theta \hat{\rho}(\theta, \phi) = 1 . \quad (2.18)$$

In what follows, we shall simplify notation and make use the abbreviations $\omega := (\theta, \phi)$ together with

$$\begin{aligned} \int d\Omega_2 &:= \int_0^{\pi/2} d\theta \int_0^{2\pi} d\phi \cos \theta \sin^3 \theta , & \implies & \int d\Omega_5 := \int d\Omega_2 \int d\Omega_3 . \\ \int d\Omega_3 &:= \int_0^{\pi/2} d\alpha \int_0^{2\pi} d\xi_1 \int_0^{2\pi} d\xi_2 \sin \alpha \cos \alpha , \end{aligned} \quad (2.19)$$

Next we wish to substitute the ansatz (2.17) into (2.13) and derive the corresponding equations of motion. To this end, we need the expression

$$|\vec{x} - \vec{x}'|^2 \Big|_{\substack{|\vec{x}| = \hat{r}(\omega) \\ |\vec{x}'| = \hat{r}(\omega')}} = \hat{r}^2(\omega) + \hat{r}^2(\omega') - 2\hat{r}(\omega)\hat{r}(\omega') \cos \varphi , \quad (2.20)$$

where φ is the angle $\angle(\frac{\vec{x}}{|\vec{x}|}, \frac{\vec{x}'}{|\vec{x}'|})$ between $\frac{\vec{x}}{|\vec{x}|}$ and $\frac{\vec{x}'}{|\vec{x}'|}$ on the five-sphere defined by

$$\begin{aligned} \cos \varphi &:= \cos \theta \cos \theta' \cos(\phi - \phi') \\ &+ \sin \theta \sin \theta' [\cos \alpha \cos \alpha' \cos(\xi_1 - \xi'_1) + \sin \alpha \sin \alpha' \cos(\xi_2 - \xi'_2)] . \end{aligned} \quad (2.21)$$

Therefore, we obtain for (2.13) (including the Lagrange multiplier term)

$$\begin{aligned} \mathcal{H}_f &= \Lambda \left(\int d\Omega_2 \hat{\rho}(\omega) - 1 \right) + N \int d\Omega_2 \hat{\rho}(\omega) [\hat{r}^2(\omega) - 2 \Re f(\hat{z})] \\ &- \frac{N^2}{8\pi^4} \int d\Omega_5 \int d\Omega'_5 \hat{\rho}(\omega) \hat{\rho}(\omega') \log [\hat{r}^2(\omega) + \hat{r}^2(\omega') - 2\hat{r}(\omega)\hat{r}(\omega') \cos \varphi] , \end{aligned} \quad (2.22)$$

where $\hat{z} = \hat{z}(\omega) = \hat{r}(\omega) \cos \theta e^{i\phi}$. Variations with respect to Λ , $\hat{\rho}$ and \hat{r} lead to the following set of equations of motion:

$$0 = \int d\Omega_2 \hat{\rho}(\omega) - 1 , \quad (2.23a)$$

$$\begin{aligned} 0 &= \frac{\Lambda}{N} + \hat{r}^2(\omega) - 2 \Re f(\hat{z}) \\ &- \frac{N}{4\pi^4} \int d\Omega_3 \int d\Omega'_5 \hat{\rho}(\omega') \log [\hat{r}^2(\omega) + \hat{r}^2(\omega')^2 - 2\hat{r}(\omega)\hat{r}(\omega') \cos \varphi] , \end{aligned} \quad (2.23b)$$

$$0 = \hat{r}(\omega) - \frac{\partial \Re f(\hat{z})}{\partial \hat{r}(\omega)} - \frac{N}{4\pi^4} \int d\Omega_3 \int d\Omega'_5 \frac{\hat{\rho}(\omega') [\hat{r}(\omega) - \hat{r}(\omega') \cos \varphi]}{\hat{r}^2(\omega) + \hat{r}^2(\omega') - 2\hat{r}(\omega)\hat{r}(\omega') \cos \varphi} . \quad (2.23c)$$

It is far from obvious how to deal with this system of integral equations in the general case. Take notice that the equations are non-linear in \hat{r} , and entangle $\hat{\rho}$ and \hat{r} in a non-trivial fashion.

Nevertheless, for the ground state wavefunction where $f = 0$, it is known that the functional \mathcal{H}_f is extremised by [7]

$$\Lambda = N^2 \Lambda_0 = N^2 (\log N + \frac{1}{12} - \log 2), \quad \hat{\rho}(\omega) = \rho_0 = \frac{2}{\pi}, \quad \hat{r}(\omega) = r_0 = \sqrt{\frac{N}{2}}. \quad (2.24)$$

This exact solution will play a key role in our subsequent discussion.

3. Analytical solutions

In this section, we will present analytical solutions to (2.23) for $f \neq 0$ and hence, the most likely distributions of eigenvalues for excited wavefunctions $\hat{\psi}_f$ (i.e. eigenfunctions of the Hamiltonian H). We shall also compare our analytical results against numerical calculations.

3.1. Perturbative expansions

The starting point for our considerations is the ground state configuration (2.24): We consider wavefunctions that can be regarded as a slight perturbation of the ground state. For them we engineer a solution to the equations of motion as a perturbative expansion around the ground state solution. For this expansion to be consistent, we must assume that the function $f = f(z)$ is ‘small’ when evaluated on solutions to (2.23), i.e. we introduce some small parameter ε and write

$$f(z) := \varepsilon r_0^2 F(z) \implies |f(z)| \ll r_0^2 = \frac{N}{2}, \quad (3.1)$$

with F being holomorphic in z . The unknowns Λ , $\hat{\rho}$ and \hat{r} are then expanded in powers of ε according to:

$$\begin{aligned} \Lambda &= N^2 (\Lambda_0 + \varepsilon \Lambda_1 + \varepsilon^2 \Lambda_2 + \dots), \\ \hat{\rho}(\omega) &= \rho_0 (1 + \varepsilon \rho_1(\omega) + \varepsilon^2 \rho_2(\omega) + \dots), \\ \hat{r}(\omega) &= r_0 (1 + \varepsilon r_1(\omega) + \varepsilon^2 r_2(\omega) + \dots), \end{aligned} \quad (3.2)$$

where Λ_0 , ρ_0 and r_0 were given in (2.24).

The equations of motion (2.23) can now be solved order by order in powers of ε to eventually arrive at a perturbative solution of the form (3.2). The upshot of this expansion is that at any given order $k + 1$ (with $k \geq 0$), the integral equations for $\rho_{k+1} = \rho_{k+1}(\omega)$ and $r_{k+1} = r_{k+1}(\omega)$ are decoupled and linearised. Specifically, upon substituting (3.2) into (2.23), a few algebraic manipulations show that

$$0 = \int d\Omega_2 \rho_{k+1}(\omega), \quad (3.3a)$$

$$P_{k+1}(\omega) = \Lambda_{k+1} - \int d\Omega'_2 K_I(\omega, \omega') \rho_{k+1}(\omega'), \quad (3.3b)$$

$$R_{k+1}(\omega) = \frac{2}{3} r_{k+1}(\omega) + \int d\Omega'_2 K_{II}(\omega, \omega') r_{k+1}(\omega'). \quad (3.3c)$$

Here, we have introduced the integral kernels

$$\begin{aligned} K_I(\omega, \omega') &:= \frac{1}{2\pi^5} \int d\Omega_3 \int d\Omega'_3 \log(1 - \cos \varphi), \\ K_{II}(\omega, \omega') &:= \frac{1}{2\pi^5} \int d\Omega_3 \int d\Omega'_3 \frac{1}{1 - \cos \varphi}. \end{aligned} \quad (3.4)$$

The remainders $P_{k+1} = P_{k+1}(\omega)$ and $R_{k+1} = R_{k+1}(\omega)$ are functions which depend only on the solutions Λ_l , ρ_l and r_l , with $l \leq k$. They can be obtained order by order and the first few expressions are

$$\begin{aligned} P_1(\omega) &= \Re \mathbf{e} F(\hat{z}) \Big|_{\hat{r}=r_0} + \frac{1}{\pi} \int d\Omega_2 R_1(\omega) , \\ R_1(\omega) &= \hat{r} \frac{\partial}{\partial \hat{r}} \Big|_{\hat{r}=r_0} \Re \mathbf{e} F(\hat{z}) \end{aligned} \quad (3.5)$$

and

$$\begin{aligned} P_2(\omega) &= \frac{1}{3} r_1^2(\omega) + \frac{1}{\pi} \int d\Omega_2 r_1(\omega) [2\rho_1(\omega) - r_1(\omega)] \\ &\quad + \frac{1}{2} \int d\Omega'_2 K_{\text{II}}(\omega, \omega') r_1^2(\omega') + \frac{1}{\pi} \int d\Omega_2 R_2(\omega) , \\ R_2(\omega) &= r_1(\omega) \left(\hat{r} \frac{\partial}{\partial \hat{r}} \right)^2 \Big|_{\hat{r}=r_0} \Re \mathbf{e} F(\hat{z}) - \frac{5}{3} r_1(\omega)^2 + r_1(\omega) \int d\Omega'_2 K_{\text{II}}(\omega, \omega') \rho_1(\omega') \\ &\quad - \frac{1}{2} \int d\Omega'_2 K_{\text{II}}(\omega, \omega') r_1(\omega') [2\rho_1(\omega') - r_1(\omega')] . \end{aligned} \quad (3.6)$$

Notice that upon integrating equation (3.3b), the coefficients Λ_{k+1} for the Lagrange multiplier Λ are given by

$$\Lambda_{k+1} = \frac{2}{\pi} \int d\Omega_2 P_{k+1}(\omega) , \quad (3.7)$$

since $\int d\Omega_2 K_{\text{I}}(\omega, \omega') = \int d\Omega'_2 K_{\text{I}}(\omega, \omega') = \text{const}$ and $\int d\Omega_2 \rho_{k+1}(\omega) = 0$; see Appendix A for more details. Hence, at any given order $k+1$, the coefficient Λ_{k+1} is determined by the solutions Λ_l , ρ_l and r_l , with $l \leq k$ and does not depend on ρ_{k+1} and r_{k+1} .

Equations (3.3b) and (3.3c) are Fredholm integral equations of the first and second kind, respectively. Such kind of integral equations can in principle be solved if the eigenfunctions of their kernels are known. We derive the eigenfunctions of $K_{\text{I}}(\omega, \omega')$ and $K_{\text{II}}(\omega, \omega')$ in Appendix A, where we also collect some facts about these kernels. Here we just give the results of these considerations. It happens to be that

$$\Psi_{m,a}(\omega) = \Theta_{m,a}(\theta) \Phi_m(\phi) , \quad (3.8a)$$

for $m \in \mathbb{Z}$ and $a \in \mathbb{N}_0$ with

$$\Theta_{m,a}(\theta) := \cos^{|m|} \theta P_a^{(1,|m|)}(\cos 2\theta) \quad \text{and} \quad \Phi_m(\phi) := \exp(im\phi) , \quad (3.8b)$$

where $P_a^{(\alpha,\beta)}$ are the Jacobi polynomials (see Appendix B for definitions and properties), are the eigenfunctions of both kernels, though with different eigenvalues:

$$\int d\Omega'_2 K_{\text{I,II}}(\omega, \omega') \Psi_{m,a}(\omega') = \lambda_{\text{I,II}}^{m,a} \Psi_{m,a}(\omega) , \quad (3.9)$$

with

$$\begin{aligned} \lambda_{\text{I}}^{m,a} &= \begin{cases} \frac{7}{12} - \log 2 & \text{for } (m, a) = (0, 0) , \\ -24 \frac{(|m| + 2a - 1)!}{(|m| + 2a + 4)!} & \text{for } (m, a) \neq (0, 0) , \end{cases} \\ \lambda_{\text{II}}^{m,a} &= 8 \frac{(|m| + 2a)!}{(|m| + 2a + 3)!} . \end{aligned} \quad (3.10)$$

Notice that the functions (3.8) form a complete orthogonal basis for functions defined on the hemisphere given by $\omega = (\theta, \phi)$; see Figure 1.

Therefore, we may expand the remainders appearing in (3.3) in terms of (3.8),

$$P_{k+1}(\omega) = \sum_{m,a} P_{k+1}^{m,a} \Psi_{m,a}(\omega) \quad \text{and} \quad R_{k+1}(\omega) = \sum_{m,a} R_{k+1}^{m,a} \Psi_{m,a}(\omega). \quad (3.11)$$

Since P_{k+1} is real, we must have $P_{k+1}^{m,a} = (P_{k+1}^{-m,a})^*$ and similarly for R_{k+1} ; ‘*’ indicates complex conjugation. Likewise, Λ_{k+1} , ρ_{k+1} and r_{k+1} can be expanded in terms of (3.8). Upon replacing all of these expansions in the integral equations (3.3), we find that Λ_{k+1} , ρ_{k+1} and r_{k+1} are given by

$$\Lambda_{k+1} = P_{k+1}^{0,0}, \quad (3.12a)$$

$$\rho_{k+1}(\omega) = - \sum_{(m,a) \neq (0,0)} \frac{P_{k+1}^{m,a}}{\lambda_I^{m,a}} \Psi_{m,a}(\omega), \quad (3.12b)$$

$$r_{k+1}(\omega) = \sum_{m,a} \frac{R_{k+1}^{m,a}}{\frac{2}{3} + \lambda_{II}^{m,a}} \Psi_{m,a}(\omega). \quad (3.12c)$$

It should be stressed that in general there is no guarantee that the expressions (3.12b) and (3.12c) would define square-integrable functions. For that to happen, the functions P_{k+1} and R_{k+1} should meet certain criteria. In particular, (3.3b) is a Fredholm integral equation of the first kind with symmetric kernel and a complete set of eigenfunctions. Therefore, certain existence theorems apply. Specifically, (3.3b) has a unique L_2 -solution given by (3.12b) if and only if the infinite series

$$\sum_{(m,a) \neq (0,0)} \left| \frac{P_{k+1}^{m,a}}{\lambda_I^{m,a}} \right|^2 \quad (3.13)$$

is convergent. For more details, see e.g. [15].

In summary, provided certain criteria are met, we are able to solve the saddle point equations (2.23) analytically by means of the perturbative expansions (3.2).

3.2. Example A: Monomial deformations

Let us now consider an example and take $f(z) \propto z^p$ for $p \in \mathbb{N}$. Firstly, these are the simplest distortions of the ground state wavefunction. Secondly, and more interestingly, these wavefunctions should correspond to simple gravitational duals. Indeed, they are expected to be in correspondence with the LLM geometries obtained from a simply connected droplet possessing a non-vanishing p^{th} harmonic moment [10].

For this to constitute a small perturbation, $f(z)$ should be of order εr_0^2 , with $\varepsilon \ll 1$. Thus, the constant of the monomial is taken to scale with N . In particular, we consider

$$f(z) = \varepsilon r_0^2 \left(\frac{z}{r_0} \right)^p \implies F(z) = \left(\frac{z}{r_0} \right)^p \quad \text{and} \quad \Re e F(z) = \left(\frac{r}{r_0} \right)^p \cos^p \theta \cos p\phi. \quad (3.14)$$

Notice that since $\Re e F(z)$ is an even function in ϕ and since $K_{I,II}(\theta, \phi, \theta', \phi') = K_{I,II}(\theta, -\phi, \theta', -\phi')$ as a direct consequence of (2.21) and (3.4), the functions $\hat{\rho}$ and \hat{r} will be even functions in ϕ . Hence, the series expansions (3.12) reduce to expansions in terms of $\Re e \Psi_{m,a}$ with $m \geq 0$ and real coefficients (i.e. we only need the $\cos m\phi$ terms in the Fourier expansion).

Therefore, the expressions (3.5) for the remainders P_1 and R_1 are given by

$$\begin{aligned} P_1(\omega) &= \cos^p \theta \cos p\phi = \Re e \Psi_{p,0}(\omega), \\ R_1(\omega) &= p \cos^p \theta \cos p\phi = p \Re e \Psi_{p,0}(\omega). \end{aligned} \quad (3.15)$$

Using these results and the series expansions (3.12), we then obtain

$$\Lambda_1 = 0 , \quad (3.16a)$$

$$\rho_1(\omega) = \frac{1}{24} \frac{(p+4)!}{(p-1)!} \cos^p \theta \cos p\phi , \quad (3.16b)$$

$$r_1(\omega) = \frac{3p(p+3)!}{2(p+3)! + 24p!} \cos^p \theta \cos p\phi . \quad (3.16c)$$

p	$\rho_2^{2p,0}$	$\rho_2^{0,0}$	$\rho_2^{0,1}$	$\rho_2^{0,2}$	$\rho_2^{0,3}$	$\rho_2^{0,4}$
2	$\frac{925}{3}$	0	10	$\frac{185}{6}$	0	0
3	$\frac{435375}{121}$	0	$\frac{2430}{121}$	$\frac{89910}{847}$	$\frac{87075}{847}$	0
4	$\frac{29458800}{1369}$	0	$\frac{40320}{1369}$	$\frac{7560}{37}$	$\frac{481600}{1369}$	$\frac{233800}{1369}$

Table 1: Coefficients of $\rho_2(\omega)$.

p	$r_2^{2p,0}$	$r_2^{0,0}$	$r_2^{0,1}$	$r_2^{0,2}$	$r_2^{0,3}$	$r_2^{0,4}$
2	$\frac{2875}{592}$	$-\frac{115}{32}$	0	$\frac{575}{1184}$	0	0
3	$\frac{42795}{1892}$	$-\frac{12681}{968}$	$-\frac{1125}{484}$	$\frac{492075}{250712}$	$\frac{8559}{13244}$	0
4	$\frac{14391825}{228623}$	$-\frac{136885}{4107}$	$-\frac{43840}{4107}$	$\frac{348705}{101306}$	$\frac{477680}{176601}$	$\frac{685325}{1371738}$

Table 2: Coefficients of $r_2(\omega)$.

Next we would like to compute the solution to order ε^2 . As it is clear from (3.6) and (3.16), in order to compute Λ_2 , ρ_2 and r_2 we need to expand $(\cos^p \theta \cos p\phi)^2 = [\Re \Psi_{p,0}(\omega)]^2$ in terms of the eigenfunctions (3.8). We find

$$[\Re \Psi_{p,0}(\omega)]^2 = \frac{1}{2} \Re \Psi_{2p,0}(\omega) + \sum_{q=0}^p \frac{(q+1)^2 p!^2}{(p-q)!(p+q+2)!} \Re \Psi_{0,q}(\omega) . \quad (3.17)$$

Therefore, using (3.6), the non-vanishing coefficients $F_2^{m,a}$ and $R_2^{m,a}$,

$$P_2(\omega) = \sum_{m,a} F_2^{m,a} \Re \Psi_{m,a}(\omega) \quad \text{and} \quad R_2(\omega) = \sum_{m,a} R_2^{m,a} \Re \Psi_{m,a}(\omega) , \quad (3.18)$$

are computed to be

$$F_2^{m,a} = \begin{cases} \frac{b_p c_{p,0}}{2} \left[p^2 + \left(\frac{2}{3} + \lambda_{\text{II}}^{p,0} \right) a_p \right] & \text{for } (m,a) = (0,0) , \\ \frac{b_p^2}{4} \left(\frac{2}{3} + \lambda_{\text{II}}^{2p,0} \right) & \text{for } (m,a) = (2p,0) , \\ \frac{b_p^2 c_{p,q}}{2} \left(\frac{2}{3} + \lambda_{\text{II}}^{0,q} \right) & \text{for } (m,a) = (0, 1 \leq q \leq p) , \end{cases} \quad (3.19a)$$

$$R_2^{m,a} = \begin{cases} \frac{b_p}{2} \left[p^2 - \frac{5}{3} b_p + a_p \lambda_{\text{II}}^{p,0} - \left(a_p - \frac{b_p}{2} \right) \lambda_{\text{II}}^{2p,0} \right] & \text{for } (m,a) = (2p,0) , \\ b_p c_{p,q} \left[p^2 - \frac{5}{3} b_p + a_p \lambda_{\text{II}}^{p,0} - \left(a_p - \frac{b_p}{2} \right) \lambda_{\text{II}}^{0,q} \right] & \text{for } (m,a) = (0, 0 \leq q \leq p) , \end{cases}$$

where

$$a_p := \frac{1}{24} \frac{(p+4)!}{(p-1)!}, \quad b_p := \frac{3p(p+3)!}{2(p+3)! + 24p!} \quad \text{and} \quad c_{p,q} := \frac{(q+1)^2 p!^2}{(p-q)!(p+q+2)!} \quad (3.19b)$$

and the eigenvalues $\lambda_{\text{I,II}}^{m,a}$ were given in (3.10). From these expressions, we obtain

$$\Lambda_2 = P_2^{0,0}, \quad \rho_2^{m,a} = -\frac{P_2^{m,a}}{\lambda_{\text{I}}^{m,a}} \quad \text{for} \quad (m,a) \neq (0,0) \quad \text{and} \quad r_2^{m,a} = \frac{R_2^{m,a}}{\frac{2}{3} + \lambda_{\text{II}}^{m,a}} \quad (3.20)$$

as the only non-vanishing coefficients appearing in

$$\rho_2(\omega) = \sum_{m,a} \rho_2^{m,a} \Re \epsilon \Psi_{m,a}(\omega) \quad \text{and} \quad r_2(\omega) = \sum_{m,a} r_2^{m,a} \Re \epsilon \Psi_{m,a}(\omega). \quad (3.21)$$

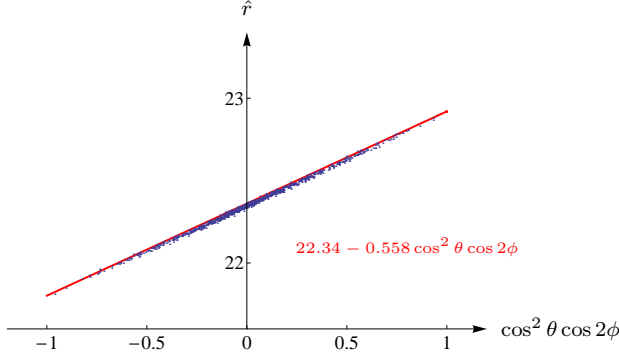
We refrain from writing down these expressions explicitly, as they are lengthy and not particularly illuminating. Instead, we only list the particular values for $p = 2, 3, 4$ in Tables 1 and 2.

In what follows, in order to compare against the analytical results, we will compute these coefficients out of numerical solutions. To have a numerical handle on the problem, we can retrace our steps from the continuum limit to finite N . For finite N , the extrema of \mathcal{H}_f will not dominate the partition function (2.11a) anymore as the saddle point approximation is only valid in the thermodynamic limit $N \rightarrow \infty$. Instead, for a finite N description, one should take into account all possible configurations weighted by their respective probability. In order to do that in a good approximation, Monte Carlo simulations with a Metropolis criterion can be used to simulate the distribution of probabilities: Starting off from a random distribution of particles, a new one is generated by a small random perturbation. The new configuration is accepted if $e^{-\delta \mathcal{H}_f}$ (where \mathcal{H}_f is the discrete Hamiltonian (2.11b)) is larger than a random number in the interval $[0, 1]$ and rejected otherwise. By iterating this algorithm a large number of times, a typical (i.e. most likely) configuration of particles will be obtained at the end. This method was used to describe different wavefunctions of the matrix model we are dealing with for finite N in works by Berenstein and collaborators [6, 12, 13].

At this point, we should emphasise that the remainder of this section is not aimed at finding the finite N description of wavefunctions. Instead, we will use the finite N problem as a discretisation of the equations of motions of the continuum limit, which, of course, would be valid in the $N \rightarrow \infty$ limit. In other words, we will consider the finite N Hamiltonians \mathcal{H}_f and still look for their extrema numerically and regard these as numerical approximations of the perturbative analytical solutions presented previously. To do that, we will simply modify the Metropolis criterion to accept new configurations only if $\delta \mathcal{H}_f < 0$. In this way, the iteration procedure will produce configurations approaching the extrema of \mathcal{H}_f . All the simulations in this work that use this modified Metropolis criterion were performed in `Mathematica`.

Using that method we obtained numerical approximations for the cases $p = 2, 3, 4$ with $\varepsilon = 0.01$. In these three cases, we discretised the densities using $N = 1000$. For such small ε , the main dependence of \hat{r} will be that of the linear order in ε . If one plots \hat{r} versus $\cos^p \theta \cos p\phi$, the points should approximately lie in a line. In Figure 2 we produce those plots on top of their linear fittings. The agreement of these numerical fittings with the analytical coefficients is very good. Certainly, beyond the the leading approximation, \hat{r} is not a function of $\cos^p \theta \cos p\phi$ only. By fitting \hat{r} as an expansion of the eigenfunctions kicking in at higher orders in ε one can obtain the corresponding numerical coefficients. For instance, for $p = 2$, we get the coefficients

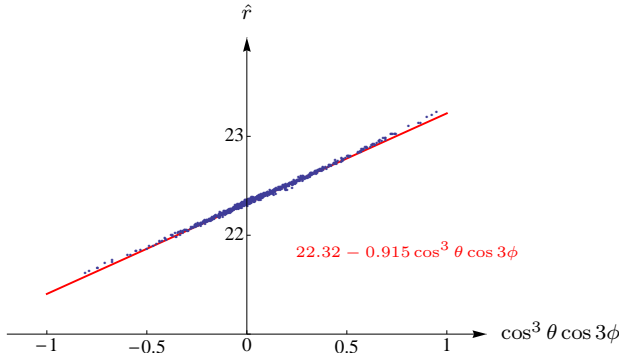
$$(r_2^{4,0}, r_2^{0,0}, r_2^{0,1}, r_2^{0,2}) \Big|_{\text{numerical}} \approx (5.1, -3.7, 0.02, 0.58) \quad (3.22a)$$



(a)

Case $p = 2$:

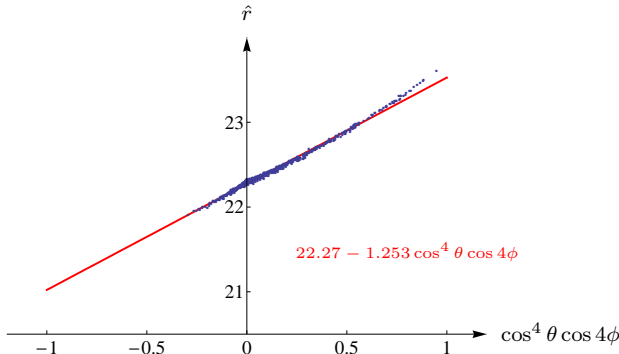
This is very close to the analytical solution $\sqrt{500}(1 - \frac{115}{32}\varepsilon^2 - \frac{5}{2}\varepsilon \cos^2 \theta \cos 2\phi) \approx 22.35 - 0.559 \cos^2 \theta \cos 2\phi$.



(b)

Case $p = 3$:

This is very close to the analytical solution $\sqrt{500}(1 - \frac{12681}{968}\varepsilon^2 - \frac{45}{11}\varepsilon \cos^3 \theta \cos 3\phi) \approx 22.33 - 0.915 \cos^3 \theta \cos 3\phi$.



(b)

Case $p = 4$:

This is still close to the analytical solution $\sqrt{500}(1 - \frac{136885}{4107}\varepsilon^2 - \frac{210}{37}\varepsilon \cos^4 \theta \cos 4\phi) \approx 22.29 - 1.269 \cos^4 \theta \cos 4\phi$. The slight deviation is due to the fact that for larger p the numerical value of the (neglected) higher-order coefficients is larger.

Figure 2: Numerical solutions for $p = 2, 3, 4$ and $\varepsilon = 0.01$ obtained with $N = 1000$. The solid curves represent linear fittings of the data points.

which are fairly close to the coefficients in first row of Table 2:

$$(r_2^{4,0}, r_2^{0,0}, r_2^{0,1}, r_2^{0,2})|_{\text{analytical}} = (\frac{2875}{592}, -\frac{115}{32}, 0, \frac{575}{1184}) \approx (4.7, -3.6, 0, 0.49). \quad (3.22b)$$

It is also possible to compute the density coefficients for the numerical solutions using⁵

$$\rho^{m,a} = \frac{1}{\mathcal{N}_{m,a}} \int d\Omega_2 \hat{\rho}(\omega) \Re \Psi_{m,a}(\omega) \rightarrow \frac{1}{\mathcal{N}_{m,a}} \frac{1}{N} \sum_{i=1}^N \Re \Psi_{m,a}(\omega_i), \quad (3.23a)$$

with the normalisation constant

$$\mathcal{N}_{m,a} := \frac{\pi}{2} \frac{(a+1)(1+\delta_{m0})}{(2a+m+2)(a+m+1)}, \quad (3.23b)$$

⁵ The $\rho^{m,a}$ s are the coefficients of the full $\hat{\rho}$, i.e. $\hat{\rho}(\omega) = \sum_{m,a} \rho^{m,a} \Re \Psi_{m,a}(\omega)$.

where δ is the Kronecker delta. For $p = 2$, we obtain

$$(\rho_1^{2,0}, \rho_2^{4,0}, \rho_2^{0,1}, \rho_2^{0,2})|_{\text{numerical}} \approx (30.1, 306, 10.1, 30.0) \quad (3.24a)$$

in good agreement with the coefficients in Table 1:

$$(\rho_1^{2,0}, \rho_2^{4,0}, \rho_2^{0,1}, \rho_2^{0,2})|_{\text{analytical}} = (30, \frac{925}{3}, 10, \frac{185}{6}) \approx (30, 308.3, 10, 30.8) . \quad (3.24b)$$

3.3. Example B: Logarithmic deformations

Let us now consider a wavefunction with a logarithmic potential $f(z) = Q \log z$. In this case, the wavefunction should correspond to the BPS operator $\det Z^Q$ [2]. In turn, this operator is believed to be dual to the annular LLM geometry whose droplet inner and outer radii are \sqrt{Q} and $\sqrt{N+Q}$, respectively.

One could expect this case to be simpler because the ϕ -dependence drops out of the problem (notice that the real part of f is independent of ϕ) and the functions \hat{r} and $\hat{\rho}$ will only depend on θ . On the other hand, the distribution cannot be regarded as a small distortion of the spherical for all values of the angle θ (since f has singularities) and therefore we cannot use (3.2) to solve the equations perturbatively.

Nevertheless, there is a simplification since for a logarithmic potential, the term $\frac{\partial \Re f}{\partial \hat{r}}$ appearing in the ‘radial’ integral equation (2.23c) does not depend on θ explicitly. Therefore, (2.23c) can be solved exactly by assuming a constant radius \hat{r} :

$$\hat{r} = r_Q = \sqrt{\frac{N}{2} + Q} . \quad (3.25)$$

To arrive at this result, we have used the constraint (2.23a) to eliminate $\hat{\rho}$. We should emphasise that this solution is an exact solution for *any* value of Q .

Pleasingly, this appears to be consistent with Monte Carlo simulations for finite values of N [6, 13]. In Figure 3, we have depicted $R_{56} := \sqrt{x_5^2 + x_6^2}$ versus $R_{1234} := \sqrt{x_1^2 + x_2^2 + x_3^2 + x_4^2}$ for $N = 2000$ particles and $Q = 20$. The plot on the left corresponds to a typical (i.e. most likely) configuration obtained from a Metropolis algorithm (as done in [6, 13]). The solid curve corresponds to $R_{1234}^2 + R_{56}^2 = r_Q^2$ with $r_Q^2 = 1020$. Of course, the agreement would improve for simulations with larger N . As before, one can modify the Metropolis criterion to accept new configurations only if $\delta \mathcal{H}_f < 0$. In this way, the iteration will produce configurations approaching the extrema of \mathcal{H}_f . As shown in right plot in Figure 3, these configurations fit very well the large- N value of the constant radius (3.25).⁶

Now that we have solved exactly the radial integral equation with (3.25), we are left with a linear integral equation for the density $\hat{\rho}(\theta)$,

$$\tilde{\Lambda} - \frac{Q}{N} \log(1 + \cos 2\theta) - \frac{\pi}{2} \int_0^{\pi/2} d\theta' \cos \theta' \sin^3 \theta' \tilde{K}_I(\theta, \theta') \hat{\rho}(\theta') = 0 , \quad (3.26a)$$

with

$$\tilde{\Lambda} := \frac{\Lambda}{N^2} + \frac{r_Q^2}{N} - \frac{Q}{N} \log \frac{r_Q^2}{2} - \log 2r_Q^2 \quad \text{and} \quad \tilde{K}_I(\theta, \theta') := \int_0^{2\pi} d\phi K_I(\omega, \omega') . \quad (3.26b)$$

⁶In fact, several simulations for different N and Q values show that the particles of extremal configurations sit at $r_Q = \sqrt{\frac{N-1}{2} + Q}$.

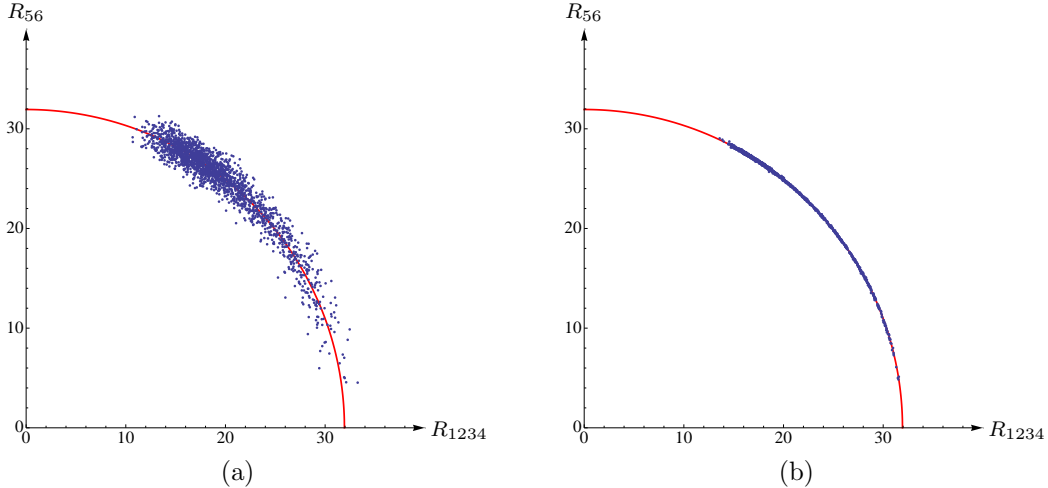


Figure 3: On the left, a typical configuration for $N = 2000$ and $Q = 20$ obtained by using a Metropolis criterion in the numerical simulation. On the right, a configuration extremising \mathcal{H}_f which is also obtained for $N = 2000$ and $Q = 20$. In both pictures, the solid curve is $R_{1234}^2 + R_{56}^2 = 1020$.

Using the expansion (A.15) of the kernel K_I , we may re-write the kernel \tilde{K}_I as an infinite series

$$\tilde{K}_I(\theta, \theta') = 4 \sum_{a=0}^{\infty} \lambda_I^{0,a} (1+a) P_a^{(1,0)}(\cos 2\theta) P_a^{(1,0)}(\cos 2\theta'), \quad (3.27)$$

where $\lambda_I^{0,a}$ was given in (3.10). Likewise, we could integrate (A.6) to arrive at an infinite series in terms of hypergeometric functions.

Equation (3.26a) is again a Fredholm integral of the first kind. In general, the range of validity of such an equation does not need to coincide with the interval of integration. In fact, (3.26a) cannot hold for all $0 \leq \theta \leq \frac{\pi}{2}$ as can be seen as follows:⁷ Firstly, (3.27) implies that \tilde{K}_I is bounded⁸ since with $|P_a^{(1,0)}(\cos 2\theta)| \leq 1+a$ for $0 \leq \theta \leq \frac{\pi}{2}$ we find

$$|\tilde{K}_I(\theta, \theta')| \leq 4 \sum_{a=0}^{\infty} |\lambda_I^{0,a}| (1+a)^3 = 4 \log 2. \quad (3.28)$$

Secondly, the integral (recall that $\hat{\rho} \geq 0$)

$$\begin{aligned} \left| \int_0^{\pi/2} d\theta' \cos \theta' \sin^3 \theta' \tilde{K}_I(\theta, \theta') \hat{\rho}(\theta') \right| &\leq \int_0^{\pi/2} d\theta' \cos \theta' \sin^3 \theta' |\tilde{K}_I(\theta, \theta')| \hat{\rho}(\theta') \\ &\leq 4 \log 2 \int_0^{\pi/2} d\theta' \cos \theta' \sin^3 \theta' \hat{\rho}(\theta') = \frac{2}{\pi} \log 2 \end{aligned} \quad (3.29)$$

is also bounded for all $0 \leq \theta \leq \frac{\pi}{2}$. In the last step of this derivation, we have used the normalisation of the density $\hat{\rho}$. However, the logarithmic term $\log(1+\cos 2\theta)$ appearing in (3.26a) is not bounded. Therefore, we conclude that (3.26a) cannot be solved for all $0 \leq \theta \leq \frac{\pi}{2}$. Note, however, that this

⁷To arrive at this conclusion, one may also argue differently. Upon expanding $\log(1+\cos 2\theta)$ and $\hat{\rho}$ in terms of the Jacobi polynomials $P_a^{(1,0)}(\cos 2\theta)$ and using (3.27), one quickly realises that the obtained series $\hat{\rho}(\theta) = \sum_a \rho_a P_a^{(1,0)}(\cos 2\theta)$ is not convergent as the coefficients ρ_a do not satisfy the criterion (3.13). Hence, no solution exists satisfying the equation for all $0 \leq \theta \leq \frac{\pi}{2}$.

⁸Alternatively, one may deduce this directly from the expressions (A.6).

does not contradict the intuition that a function $\hat{\rho}$ extremising \mathcal{H}_f should exist. Rather, since $\hat{\rho} \geq 0$, the extrema of \mathcal{H}_f could lie in the *boundary* of the space of the allowed configurations $\hat{\rho}$. Indeed, the above analysis indicates that the extrema of \mathcal{H}_f must be found in the boundary of the configuration space, i.e. the density $\hat{\rho}$ has to vanish in some region $U \subset [0, \frac{\pi}{2}]$ and in this region U , the integral equation will not hold.

This is consistent with the numerical simulations, where $\hat{\rho}$ appears to be vanishing in the region $U_{\theta_0} = \{\theta \mid \theta_0 \leq \theta \leq \frac{\pi}{2}\}$ for some θ_0 . Altogether, we are left with the following (one-dimensional) integral equation for $\hat{\rho}$:

$$\tilde{\Lambda} - \frac{Q}{N} \log(1 + \cos 2\theta) - \frac{\pi}{2} \int_0^{\theta_0} d\theta' \cos \theta' \sin^3 \theta' \tilde{K}_I(\theta, \theta') \hat{\rho}(\theta') = 0, \quad \text{for } 0 \leq \theta \leq \theta_0 \quad (3.30)$$

for some value $\theta_0 = \theta_0(\frac{Q}{N})$ which one has to determine consistently together with $\hat{\rho}$.⁹ To find θ_0 and $\hat{\rho}$, one should solve (3.30) for generic θ_0 (not for all θ_0 a solution should be found). Among those solutions, one then should look for the one that extremises \mathcal{H}_f .

Unfortunately, solving the Fredholm integral equation (3.30) for arbitrary θ_0 is a very difficult problem. So far, we have not been able solve the eigenvalue problem of the kernel (3.26b) for any other value than $\theta_0 = \frac{\pi}{2}$. For that reason, we shall determine $\hat{\rho}$ numerically in the following.

Let us first make a change of coordinates according to $x := \cos 2\theta$, so that the normalisation and the integral equation (3.30) read as ($x_0 := \cos 2\theta_0$):

$$0 = \int_{x_0}^1 dx (1-x) \hat{\rho}(x) - \frac{4}{\pi}, \quad (3.31a)$$

$$0 = \tilde{\Lambda} - \frac{Q}{N} \log(1+x) - \frac{\pi}{16} \int_{x_0}^1 dx' (1-x') \tilde{K}_I(x, x') \hat{\rho}(x'). \quad (3.31b)$$

These equations can be obtained from variations of¹⁰

$$\begin{aligned} \tilde{\mathcal{H}}_f = & \tilde{\Lambda} \left(\int_{-1}^1 dx (1-x) \hat{\rho}(x) - \frac{4}{\pi} \right) - \frac{Q}{N} \int_{-1}^1 dx (1-x) \log(1+x) \hat{\rho}(x) \\ & - \frac{\pi}{32} \int_{-1}^1 dx (1-x) \int_{-1}^1 dx' (1-x') \tilde{K}_I(x, x') \hat{\rho}(x) \hat{\rho}(x'). \end{aligned} \quad (3.32)$$

Note that the full range $-1 \leq x \leq 1$ is used in $\tilde{\mathcal{H}}_f$. The restriction to $x_0 \leq x \leq 1$ will be produced for configurations of $\hat{\rho}$ that exactly vanish for $x < x_0$.

To extremise $\tilde{\mathcal{H}}$, we can discretise the problem by thinking of a large number L of ‘particles’ in the interval $[-1, 1]$ and trading back integrals into sums

$$\int_{-1}^1 dx (1-x) \hat{\rho}(x) \rightarrow \frac{4}{\pi L} \sum_{i=1}^L \quad (3.33)$$

and hence,

$$\tilde{\mathcal{H}}_f = -\frac{Q}{N} \frac{4}{\pi L} \sum_{i=1}^L \log(1+x_i) - \frac{1}{2\pi L^2} \sum_{i,j=1}^L \tilde{K}_I(x_i, x_j). \quad (3.34)$$

To obtain the extrema of $\tilde{\mathcal{H}}_f$, we now perform Monte Carlo simulations with a modified Metropolis criterion (i.e. we only accept new configurations if $\delta \tilde{\mathcal{H}}_f < 0$). The big advantage of

⁹Notice that $\theta_0(\frac{Q}{N} = 0) = \frac{\pi}{2}$. Furthermore, a necessary condition is that $|\tilde{\Lambda} - \frac{Q}{N} \log(1 + \cos 2\theta_0)| \leq \log 2$ as follows from (3.29).

¹⁰Notice that $\tilde{\mathcal{H}}_f$ is basically a redefinition of \mathcal{H}_f .

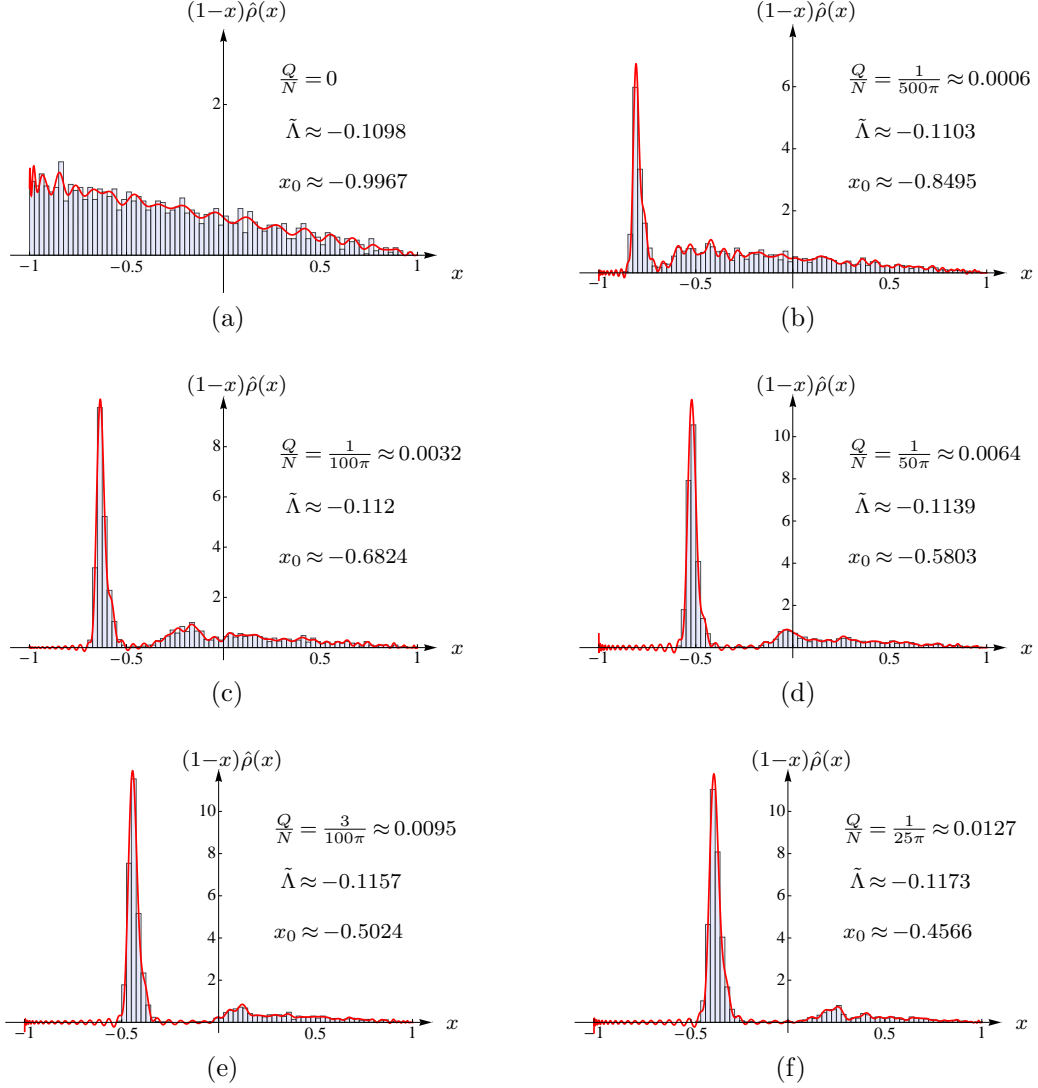


Figure 4: Numerical solutions for $(1-x)\hat{\rho}(x)$ for various values of $\frac{Q}{N}$. The number L of ‘particles’ for doing the numerics is always 2000. The solid line represents an interpolating function obtained by numerically expanding the solutions $\hat{\rho}$ in terms of the Jacobi polynomials. Notice that the analytical result for $\frac{Q}{N} = 0$ is $\hat{\rho}(x) = \frac{2}{\pi} \approx 0.6366$, $\tilde{\Lambda} = \frac{7}{12} - \log 2 \approx -0.1098$ and $x_0 = -1$. The small oscillations are an artifact of the discretisation: They become smaller as L is taken larger. These results agree with those found previously in [6, 13].

the numerical approach considered here when compared to the one for the original Hamiltonian (2.11b) is that we have effectively reduced the six-dimensional problem to a one-dimensional problem. However, there is also a slight disadvantage in that the interaction term appearing in $\tilde{\mathcal{H}}_f$ is more complicated. Notice that the numerical value for the Lagrange multiplier $\tilde{\Lambda}$ (and thus Λ via (3.26b)) can be found from the discretised version of (3.31):

$$0 = \tilde{\Lambda} - \frac{Q}{N} \log(1+x_i) - \frac{1}{4L} \sum_{j=1}^L \tilde{K}_I(x_i, x_j). \quad (3.35)$$

Notice also that this equation can be used as a criterion to estimate how good our numerical solutions are (since $\tilde{\Lambda}$ should be constant for all x_i). In Figure 4, we have depicted our numerical results for various values of $\frac{Q}{N}$. The number L of ‘particles’ was chosen to be 2000.

4. Conclusions and outlook

We have considered a particular quantum mechanics model of commuting matrices which is believed to describe 1/8 BPS states in $SU(N)$ $\mathcal{N} = 4$ SYM theory at strong coupling. The wavefunctions of this model are expected to be dual to type IIB supergravity solutions that asymptotically approach $AdS_5 \times S^5$. The probability densities for the wavefunctions are interpreted as partition functions of certain matrix models. Different wavefunctions correspond to different potentials in the associated matrix model Hamiltonian.

Specifically, we focused on the large- N or thermodynamic limit in which the probability densities are dominated by the saddle points of the matrix model. Then, we have solved analytically the saddle point equations for a family of wavefunctions that are in correspondence with specific LLM geometries.

The starting point of our consideration was the ansatz (2.17), where it is assumed that the probability densities are supported on particular hypersurfaces in \mathbb{R}^6 . We then constructed a perturbative approach that allows for an analytical treatment of the saddle point equations. We used monomial potentials to illustrate how the perturbative method works. By perturbing around the ground state solution, we constructed the solution up to and including second order in the deformation parameter.

We then considered a logarithmic potential, which does not admit a perturbative solution to its saddle point equations. In spite of that, we could also obtain partial analytical results in this case. We found an exact solution (3.25), which holds true for any value of Q , for the radial function of the ansatz (2.17) and we reduced the problem to a linear integral equation for the density $\hat{\rho}$ (3.30). To provide a full analytical solution in the logarithmic case, one should diagonalise the integral kernel given in (3.26b) for a generic interval $0 \leq \theta \leq \theta_0$ with $\theta_0 < \frac{\pi}{2}$. Finally, we have compared all our analytical results against numerical simulations and found very good agreement.

The main issue which we have not discussed here but we hope to report on in the future concerns the extraction of geometry from our analytic solutions. Recall that for the ground state solution, the saddle point configuration is given by a uniform probability distribution supported on a five-sphere in \mathbb{R}^6 and an explicit geometrical meaning to this five-sphere was given in [2, 7]. The generalization of this identification is not that obvious for the excited wavefunctions. To begin with, the dual LLM geometries do not have a factorised five-dimensional compact geometry. Put it differently, the compact factor is different for different sections of the LLM geometry. At least one would expect to be able to reproduce the geometry of the section corresponding to the LLM plane. Then, there is also the question of how to read geometry out of the distribution of eigenvalues. There is obviously the hypersurface where the density is supported, but the density function must also enter somehow. For instance, although the supporting hypersurface in the logarithmic is a five-sphere, the compact factor in the LLM plane of the annular LLM solution ought to be something else.

It would also be interesting to extend our perturbative method to solve analytically the saddle point equations of more general wavefunctions. For instance, potentials that depend also on other holomorphic coordinates are supposed to describe wavefunctions of 1/4 and 1/8 BPS states. This would shed light on the AdS/CFT dictionary for those cases (see e.g. [16] and references therein). In addition, it would be very interesting to use our perturbative method to characterise excited wavefunctions in other matrix quantum mechanical systems [4, 5], which according to the AdS/CFT correspondence are dual to supergravity solutions with other asymptotics (e.g. $AdS_5 \times T^{1,1}$).

Acknowledgements. We are very grateful to D. Berenstein for important discussions and for sharing the C++ code used to create Figure 3a). D.H.C. was supported in parts by the Seventh Framework Programme under grant agreement number PIEF-GA-2008-220702. M.W. was supported by an STFC Postdoctoral Fellowship and by a Senior Research Fellowship at the Wolfson College, Cambridge, U.K.

Appendices

A Eigenvalues and eigenfunctions

In this appendix, we shall derive the eigenvalues and eigenfunctions of the kernels K_I and K_{II} introduced in (3.4). Before tackling the problem, we begin with some preliminary considerations.

Preliminaries

In the definition (3.4) of the kernels K_I and K_{II} , we are integrating over (α, ξ_1, ξ_2) and $(\alpha', \xi'_1, \xi'_2)$, i.e. over all possible positions of two points on a three-sphere. The dependence of φ on them is through the relative angle between two points on the three-sphere, so we can fix one of the points arbitrarily (say $\alpha' = 0$ and $\xi'_1 = 0$) and multiply by the volume, $2\pi^2$, of the three-sphere. In the mentioned choice, also the integral over ξ_2 becomes trivial and we obtain

$$\begin{aligned} K_I(\omega, \omega') &= \frac{2}{\pi^2} \int_0^{\pi/2} d\alpha \int_0^{2\pi} d\xi_1 \sin \alpha \cos \alpha \log(1 - \cos \varphi_0) , \\ K_{II}(\omega, \omega') &= \frac{2}{\pi^2} \int_0^{\pi/2} d\alpha \int_0^{2\pi} d\xi_1 \sin \alpha \cos \alpha \frac{1}{1 - \cos \varphi_0} \end{aligned} \quad (\text{A.1a})$$

where

$$\cos \varphi_0 := \cos \theta \cos \theta' \cos(\phi - \phi') + \sin \theta \sin \theta' \cos \alpha \cos \xi_1 . \quad (\text{A.1b})$$

There are two (equivalent) ways of computing (A.1a). Firstly, we may expand the expressions $\log(1 - \cos \varphi_0)$ and $1/(1 - \cos \varphi_0)$ in powers of $\cos \varphi_0$:

$$K_I(\omega, \omega') = - \sum_{j=1}^{\infty} \frac{1}{j} K_j(\omega, \omega') \quad \text{and} \quad K_{II}(\omega, \omega') = \sum_{j=0}^{\infty} K_j(\omega, \omega') , \quad (\text{A.2a})$$

with

$$K_j(\omega, \omega') := \frac{2}{\pi^2} \int_0^{\pi/2} d\alpha \int_0^{2\pi} d\xi_1 \sin \alpha \cos \alpha \cos^j \varphi_0 . \quad (\text{A.2b})$$

A short calculation reveals that

$$K_j(\omega, \omega') = \frac{2}{\pi} [\cos \theta \cos \theta' \cos(\phi - \phi')]^j {}_2F_1 \left(\frac{1-j}{2}, \frac{-j}{2}; 2; \frac{\tan^2 \theta \tan^2 \theta'}{\cos^2(\phi - \phi')} \right) , \quad (\text{A.3})$$

where ${}_2F_1$ is the hypergeometric function. Notice that either the first or the second argument of the hypergeometric function appearing in (A.3) is a non-positive integer. This implies that ${}_2F_1(\frac{1-j}{2}, \frac{-j}{2}; 2; \cdot)$ is actually a polynomial in the last argument.

As an alternative to the above expansions, one may perform the integrals in (A.1a) directly. In particular, they can be re-written as

$$\begin{aligned} K_I(\omega, \omega') &= \frac{2}{\pi^2} \int_0^1 dt \int_0^{2\pi} d\xi_1 t \log(A - B t \cos \xi_1) , \\ K_{II}(\omega, \omega') &= \frac{2}{\pi^2} \int_0^1 dt \int_0^{2\pi} d\xi_1 \frac{t}{A - B t \cos \xi_1} , \end{aligned} \quad (\text{A.4a})$$

where

$$A = A(\omega, \omega') := 1 - \cos \theta \cos \theta' \cos(\phi - \phi') \quad \text{and} \quad B = B(\omega, \omega') := \sin \theta \sin \theta'. \quad (\text{A.4b})$$

Notice that $|B/A| \leq 1$ for all (ω, ω') . Using ($|\alpha| \leq 1$)

$$\begin{aligned} \int_0^{2\pi} dx \log(1 - \alpha \cos x) &= 2\pi \log \frac{1}{2} (1 + \sqrt{1 - \alpha^2}), \\ \int_0^{2\pi} dx \frac{1}{1 - \alpha \cos x} &= \frac{2\pi}{\sqrt{1 - \alpha^2}}, \end{aligned} \quad (\text{A.5})$$

the kernels (A.4a) are given by

$$\begin{aligned} K_{\text{I}}(\omega, \omega') &= \frac{2}{\pi} \left[\log \frac{1}{2} (A + \sqrt{A^2 - B^2}) - \frac{1}{2} + \frac{A}{B^2} (A - \sqrt{A^2 - B^2}) \right] \\ &= \frac{2}{\pi} \left[\log A - \frac{B^2}{8A^2} {}_3F_2 \left(1, 1, \frac{3}{2}; 2, 3; \frac{B^2}{A^2} \right) \right], \\ K_{\text{II}}(\omega, \omega') &= \frac{2}{\pi} \frac{2}{B^2} (A - \sqrt{A^2 - B^2}) \\ &= \frac{2}{\pi} \frac{1}{A} {}_2F_1 \left(\frac{1}{2}, 1; 2; \frac{B^2}{A^2} \right), \end{aligned} \quad (\text{A.6})$$

where ${}_3F_2$ is a generalised hypergeometric function.

Notice that as a by-product we have obtained the non-trivial identities

$$\begin{aligned} - \sum_{j=1}^{\infty} \frac{1}{j} x^j {}_2F_1 \left(\frac{1-j}{2}, \frac{-j}{2}; 2; y^2 \right) &= \log(1-x) - \frac{x^2 y^2}{8(1-x)^2} {}_3F_2 \left(1, 1, \frac{3}{2}; 2, 3; \frac{x^2 y^2}{(1-x)^2} \right), \\ \sum_{j=0}^{\infty} x^j {}_2F_1 \left(\frac{1-j}{2}, \frac{-j}{2}; 2; y^2 \right) &= \frac{1}{1-x} {}_2F_1 \left(\frac{1}{2}, 1; 2; \frac{x^2 y^2}{(1-x)^2} \right) \end{aligned} \quad (\text{A.7})$$

between hypergeometric functions.

Eigenvalue problem

Let us now derive the eigenvalues and eigenfunctions for the kernels K_{I} and K_{II} . To this end, the form (A.2) turns out to be very adequate, since the sub-kernels (A.3) can actually be diagonalised simultaneously.¹¹ In fact,

$$\int d\Omega'_2 K_j(\omega, \omega') \Psi_{m,a}(\omega') = \underbrace{\frac{(1 + (-1)^{|m|+j}) 2^{-j} \Gamma(j+1)}{\Gamma(\frac{j}{2} - \frac{|m|}{2} - a + 1) \Gamma(\frac{j}{2} + \frac{|m|}{2} + a + 3)}}_{=: \lambda_j^{m,a}} \Psi_{m,a}(\omega), \quad (\text{A.8a})$$

where

$$\Psi_{m,a}(\omega) = \cos^{|m|} \theta P_a^{(1,|m|)}(\cos 2\theta) \exp(im\phi) \quad (\text{A.8b})$$

for $m \in \mathbb{Z}$ and $a \in \mathbb{N}_0$. Here, $P_a^{(\alpha,\beta)}$ are the Jacobi polynomials (see Appendix B) and Γ denotes the Gamma function.

¹¹Therefore, any kernel of the form $\sum_j a_j K_j$ with some constant coefficients a_j can be diagonalised in this manner.

These eigenfunctions form a complete orthogonal basis for functions defined on the hemisphere given by ω ; see Figure 1. Indeed, upon introducing the delta function

$$\delta(\omega, \omega') := \frac{\pi}{2} \frac{1}{\sin^3 \theta \cos \theta} \delta(\theta - \theta') \delta(\phi - \phi'), \quad \text{with} \quad \frac{2}{\pi} \int d\Omega'_2 \delta(\omega, \omega') = 1, \quad (\text{A.9})$$

the completeness relation is given by

$$\sum_{m,a} \frac{(|m| + 2a + 2)(|m| + a + 1)}{2a + 2} \Psi_{m,a}(\omega) [\Psi_{m,a}(\omega')]^* = \delta(\omega, \omega'), \quad (\text{A.10})$$

where ‘*’ denotes complex conjugation. This follows from the completeness relation (B.21) of the Jacobi polynomials. Furthermore, the orthogonality relation reads as

$$\frac{2}{\pi} \int d\Omega_2 \Psi_{m,a}(\omega) [\Psi_{n,b}(\omega)]^* = \frac{2a + 2}{(|m| + 2a + 2)(|m| + a + 1)} \delta_{mn} \delta_{ab}, \quad (\text{A.11})$$

where δ is the Kronecker delta. This expression can be obtained from the orthogonality relation (B.20) of the Jacobi polynomials. Altogether, we may obtain an orthonormal basis by setting

$$\Psi_{m,a}(\omega) \mapsto \Psi_{m,a}^0(\omega) := \sqrt{\frac{(|m| + 2a + 2)(|m| + a + 1)}{2a + 2}} \Psi_{m,a}(\omega) \quad (\text{A.12})$$

for which we have

$$\sum_{m,a} \Psi_{m,a}^0(\omega) [\Psi_{m,a}^0(\omega')]^* = \delta(\omega, \omega') \quad \text{and} \quad \frac{2}{\pi} \int d\Omega_2 \Psi_{m,a}^0(\omega) [\Psi_{n,b}^0(\omega)]^* = \delta_{mn} \delta_{ab}. \quad (\text{A.13})$$

Next we would like to derive the eigenvalues $\lambda_{\text{I,II}}^{m,a}$. They are given by summing up the eigenvalues $\lambda_j^{m,a}$ appearing in (A.8):

$$\lambda_{\text{I}}^{m,a} = -\sum_{j=1}^{\infty} \frac{1}{j} \lambda_j^{m,a} = \begin{cases} \frac{7}{12} - \log 2 & \text{for } (m, a) = (0, 0), \\ -24 \frac{(|m| + 2a - 1)!}{(|m| + 2a + 4)!} & \text{for } (m, a) \neq (0, 0), \end{cases} \quad (\text{A.14})$$

$$\lambda_{\text{II}}^{m,a} = \sum_{j=0}^{\infty} \lambda_j^{m,a} = 8 \frac{(|m| + 2a)!}{(|m| + 2a + 3)!}.$$

Using the eigenvalues $\lambda_{\text{I,II}}^{m,a}$ and the normalised eigenfunctions $\Psi_{m,a}^0$, the integral kernels K_{I} and K_{II} may be expressed as

$$K_{\text{I,II}}(\omega, \omega') = \frac{2}{\pi} \sum_{m,a} \lambda_{\text{I,II}}^{m,a} \Psi_{m,a}^0(\omega) [\Psi_{m,a}^0(\omega')]^*. \quad (\text{A.15})$$

Notice that upon using (A.6), one easily computes the traces $\text{tr } K_{\text{I}}$ and $\text{tr } K_{\text{II}}$. They can also be obtained by summing up the eigenvalues (A.14):

$$\text{tr } K_{\text{I,II}} = \int d\Omega_2 K_{\text{I,II}}(\omega, \omega) = \sum_{m,a} \lambda_{\text{I,II}}^{m,a} = \begin{cases} -\log 2, \\ 4. \end{cases} \quad (\text{A.16})$$

B Jacobi polynomials

The Jacobi polynomials $P_a^{(\alpha,\beta)}$ for $\alpha, \beta \in \mathbb{R}$ (with $\alpha, \beta > -1$) and $a \in \mathbb{N}_0$ are solutions to the ordinary differential equation

$$(1-x^2)y'' + (\beta - \alpha - (\alpha + \beta + 2)x)y' + a(a + \alpha + \beta + 1)y = 0 \quad (\text{B.17})$$

and they can be obtained from the hypergeometric function ${}_2F_1$ according to

$$P_a^{(\alpha,\beta)}(x) = \frac{(\alpha+1)_a}{a!} {}_2F_1\left(-a, 1 + \alpha + \beta + a; \alpha + 1; \frac{1-x}{2}\right), \quad (\text{B.18})$$

where $(a)_n := \Gamma(a+n)/\Gamma(a)$ is the Pochhammer symbol. We are particularly interested in the polynomials $P_a^{(1,m)}$ which are:

$$\begin{aligned} P_0^{(1,m)}(x) &= 1, \\ P_1^{(1,m)}(x) &= 2 + \frac{1}{2}(3+m)(x-1), \\ P_2^{(1,m)}(x) &= 3 + \frac{3}{2}(4+m)(x-1) + \frac{1}{8}(4+m)(5+m)(x-1)^2, \\ P_3^{(1,m)}(x) &= 4 + 3(5+m)(x-1) + \frac{1}{2}(5+m)(6+m)(x-1)^2 \\ &\quad + \frac{1}{48}(5+m)(6+m)(7+m)(x-1)^3, \\ &\vdots \end{aligned} \quad (\text{B.19})$$

Furthermore, the Jacobi polynomials form an orthogonal basis with

$$\int_{-1}^1 dx (1-x)^\alpha (1+x)^\beta P_a^{(\alpha,\beta)}(x) P_b^{(\alpha,\beta)}(x) = \frac{2^{\alpha+\beta+1}}{2a + \alpha + \beta + 1} \frac{(a+1)_\alpha}{(\beta+a+1)_\alpha} \delta_{ab}. \quad (\text{B.20})$$

The completeness relation is given by

$$\sum_{a=0}^{\infty} \frac{(\alpha + \beta + 2a + 1)(\beta + a + 1)_\alpha}{(a+1)_\alpha} P_a^{(\alpha,\beta)}(x) P_a^{(\alpha,\beta)}(y) = \frac{2^{\alpha+\beta+1}}{(1-x)^\alpha (1+x)^\beta} \delta(x-y) \quad (\text{B.21})$$

for $|x| < 1$ and $|y| < 1$.

Finally, we record the following useful relations:

$$P_a^{(\alpha,\beta)}(-x) = (-1)^a P_a^{(\beta,\alpha)}(x) \quad (\text{B.22})$$

and

$$\frac{d^k}{dx^k} P_a^{(\alpha,\beta)}(x) = \frac{(\alpha + \beta + a + 1)_k}{2^k} P_{a-k}^{(\alpha+k,\beta+k)}(x). \quad (\text{B.23})$$

References

- [1] J. M. Maldacena, “*The large- N limit of superconformal field theories and supergravity*”, *Adv. Theor. Math. Phys.* 2, 231 (1998), [hep-th/9711200](#). • S. S. Gubser, I. R. Klebanov and A. M. Polyakov, “*Gauge theory correlators from non-critical string theory*”, *Phys. Lett.* B428, 105 (1998), [hep-th/9802109](#). • E. Witten, “*Anti-de Sitter space and holography*”, *Adv. Theor. Math. Phys.* 2, 253 (1998), [hep-th/9802150](#).
- [2] D. Berenstein, “*Large- N BPS states and emergent quantum gravity*”, *JHEP* 0601, 125 (2006), [hep-th/0507203](#).

- [3] D. E. Berenstein, M. Hanada and S. A. Hartnoll, “*Multi-matrix models and emergent geometry*”, JHEP 0902, 010 (2009), [arxiv:0805.4658](#).
- [4] D. Berenstein and D. H. Correa, “*Emergent geometry from q -deformations of $\mathcal{N} = 4$ super Yang–Mills*”, JHEP 0608, 006 (2006), [hep-th/0511104](#). • D. Berenstein and R. Cotta, “*Aspects of emergent geometry in the AdS/CFT context*”, Phys. Rev. D74, 026006 (2006), [hep-th/0605220](#).
- [5] D. Berenstein, “*Strings on conifolds from strong coupling dynamics, part I*”, JHEP 0804, 002 (2008), [arxiv:0710.2086](#). • D. E. Berenstein and S. A. Hartnoll, “*Strings on conifolds from strong coupling dynamics: quantitative results*”, JHEP 0803, 072 (2008), [arxiv:0711.3026](#).
- [6] D. Berenstein and R. Cotta, “*A Monte Carlo study of the AdS/CFT correspondence: An exploration of quantum gravity effects*”, JHEP 0704, 071 (2007), [hep-th/0702090](#).
- [7] D. Berenstein, D. H. Correa and S. E. Vazquez, “*All loop BMN state energies from matrices*”, JHEP 0602, 048 (2006), [hep-th/0509015](#).
- [8] S. Corley, A. Jevicki and S. Ramgoolam, “*Exact correlators of giant gravitons from dual $\mathcal{N} = 4$ SYM theory*”, Adv. Theor. Math. Phys. 5, 809 (2002), [hep-th/0111222](#). • D. Berenstein, “*A toy model for the AdS/CFT correspondence*”, JHEP 0407, 018 (2004), [hep-th/0403110](#). • Y. Takayama and A. Tsuchiya, “*Complex matrix model and fermion phase space for bubbling AdS geometries*”, JHEP 0510, 004 (2005), [hep-th/0507070](#). • A. Donos, A. Jevicki and J. P. Rodrigues, “*Matrix model maps in AdS/CFT*”, Phys. Rev. D72, 125009 (2005), [hep-th/0507124](#). • R. d. M. Koch and J. Murugan, “*Emergent space-time*”, [arxiv:0911.4817](#).
- [9] H. Lin, O. Lunin and J. M. Maldacena, “*Bubbling AdS space and 1/2 BPS geometries*”, JHEP 0410, 025 (2004), [hep-th/0409174](#).
- [10] S. E. Vazquez, “*Reconstructing 1/2 BPS space-time metrics from matrix models and spin chains*”, Phys. Rev. D75, 125012 (2007), [hep-th/0612014](#).
- [11] H.-Y. Chen, D. H. Correa and G. A. Silva, “*Geometry and topology of bubble solutions from gauge theory*”, Phys. Rev. D76, 026003 (2007), [hep-th/0703068](#). • R. de Mello Koch, “*Geometries from Young diagrams*”, JHEP 0811, 061 (2008), [arxiv:0806.0685](#). • R. de Mello Koch, T. K. Dey, N. Ives and M. Stephanou, “*Hints of Integrability Beyond the Planar Limit*”, JHEP 1001, 014 (2010), [arxiv:0911.0967](#). • H. Lin, A. Morisse and J. P. Shock, “*Strings on Bubbling Geometries*”, JHEP 1006, 055 (2010), [arxiv:1003.4190](#).
- [12] D. Berenstein, R. Cotta and R. Leonardi, “*Numerical tests of AdS/CFT at strong coupling*”, Phys. Rev. D78, 025008 (2008), [arxiv:0801.2739](#).
- [13] D. Berenstein and Y. Nakada, “*The shape of emergent quantum geometry from an $\mathcal{N} = 4$ SYM minisuperspace approximation*”, [arxiv:1001.4509](#).
- [14] E. Brezin, C. Itzykson, G. Parisi and J. B. Zuber, “*Planar diagrams*”, Commun. Math. Phys. 59, 35 (1978).
- [15] F. G. Tricomi, “*Integral equations*”, Pure Appl. Math. V, Interscience, London, 1957.
- [16] B. Chen, S. Cremonini, A. Donos, F.-L. Lin, H. Lin, J. T. Liu, D. Vaman and W.-Y. Wen, “*Bubbling AdS and droplet descriptions of BPS geometries in IIB supergravity*”, JHEP 0710, 003 (2007), [arxiv:0704.2233](#).